

MIT Open Access Articles

Microscale structural model of Alzheimer A β (1-40) amyloid fibril

The MIT Faculty has made this article openly available. **Please share** how this access benefits you. Your story matters.

Citation: Paparcone, Raffaella, and Markus J. Buehler. "Microscale Structural Model of Alzheimer A β (1-40) Amyloid Fibril." *Applied Physics Letters* 94.24 (2009): 243904. © 2009 American Institute of Physics

As Published: <http://dx.doi.org/10.1063/1.3148641>

Publisher: American Institute of Physics (AIP)

Persistent URL: <http://hdl.handle.net/1721.1/77244>

Version: Final published version: final published article, as it appeared in a journal, conference proceedings, or other formally published context

Terms of Use: Article is made available in accordance with the publisher's policy and may be subject to US copyright law. Please refer to the publisher's site for terms of use.



Microscale structural model of Alzheimer A β (1–40) amyloid fibril

Raffaella Paparcone and Markus J. Buehler

Citation: *Appl. Phys. Lett.* **94**, 243904 (2009); doi: 10.1063/1.3148641

View online: <http://dx.doi.org/10.1063/1.3148641>

View Table of Contents: <http://apl.aip.org/resource/1/APPLAB/v94/i24>

Published by the [American Institute of Physics](#).

Related Articles

Separated topologies—A method for relative binding free energy calculations using orientational restraints
JCP: BioChem. Phys. **7**, 02B614 (2013)

Separated topologies—A method for relative binding free energy calculations using orientational restraints
J. Chem. Phys. **138**, 085104 (2013)

Reduced atomic pair-interaction design (RAPID) model for simulations of proteins
JCP: BioChem. Phys. **7**, 02B605 (2013)

Reduced atomic pair-interaction design (RAPID) model for simulations of proteins
J. Chem. Phys. **138**, 064102 (2013)

Generalized Born forces: Surface integral formulation
JCP: BioChem. Phys. **7**, 02B603 (2013)

Additional information on *Appl. Phys. Lett.*

Journal Homepage: <http://apl.aip.org/>

Journal Information: http://apl.aip.org/about/about_the_journal

Top downloads: http://apl.aip.org/features/most_downloaded

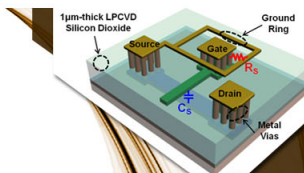
Information for Authors: <http://apl.aip.org/authors>

ADVERTISEMENT



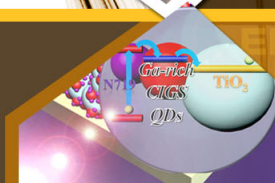
**EXPLORE WHAT'S
NEW IN APL**

SUBMIT YOUR PAPER NOW!



SURFACES AND INTERFACES

Focusing on physical, chemical, biological, structural, optical, magnetic and electrical properties of surfaces and interfaces, and more...



ENERGY CONVERSION AND STORAGE

Focusing on all aspects of static and dynamic energy conversion, energy storage, photovoltaics, solar fuels, batteries, capacitors, thermoelectrics, and more...

Microscale structural model of Alzheimer $A\beta(1-40)$ amyloid fibril

Raffaella Paparcone and Markus J. Buehler^{a)}

Department of Civil and Environmental Engineering, Laboratory for Atomistic and Molecular Mechanics, Massachusetts Institute of Technology, 77 Massachusetts Ave. Room 1-235A&B, Cambridge, Massachusetts 02139, USA

(Received 29 April 2009; accepted 12 May 2009; published online 16 June 2009)

Amyloid fibril formation and characterization are crucial due to their association with severe degenerative disorders such as Alzheimer's, type II diabetes, and Parkinson's disease. Here we present an atomistic-based multiscale analysis, utilized to predict the structure of Alzheimer $A\beta(1-40)$ fibrils. Our study provides a structural model of amyloid fibers with lengths of hundreds of nanometers at atomistic resolution. We report a systematic analysis of the energies, structural changes and H-bonding for varying fibril lengths, elucidating their size dependent properties. Our model predicts the formation of twisted amyloid microfibers with a periodicity of ≈ 82 nm, in close agreement with experimental results. © 2009 American Institute of Physics.

[DOI: 10.1063/1.3148641]

Amyloids are hierarchical protein materials, formed by insoluble fibrous protein aggregates observed in connection with severe degenerative disorders^{1,2} [Fig. 1(a)]. It has been shown that a great variety of amino acid sequences can lead to the formation of amyloid fibers, provided they share some characteristic features such as an elongated, unbranched morphology, as well as a core structure that consists of a set of β -sheets oriented in parallel to the fibril axis, with their strands perpendicular to this axis.³ Recent progress in the application of solid state NMR⁴⁻⁶ and in growing elongated amyloid microcrystals has provided detailed structural and biochemical information on the molecular-level structure amyloids.³ In particular, these studies revealed that the molecules composing the fibrils possess a degree of uniformity that has previously only been associated with crystalline materials. However, many of their fundamental physical properties, specifically their great strength, sturdiness and elasticity, are not fully understood. This is partly due to the fact that larger-scale structural models of amyloid fibrils remain elusive, preventing bottom-up studies to describe the link between their hierarchical structure and physical properties. In this letter we apply a novel method for the prediction of amyloid fiber geometries based on energetic and geometrical considerations, providing the missing detailed atomistic structures of long amyloid fibers at scales of hundreds of nanometers, resulting in a direct link between the atomistic level and the microscale [Fig. 1(a)].

Here we focus on amyloid fibrils formed by the β -amyloid peptide $A\beta(1-42)$ associated with Alzheimer's disease.^{4,7} A molecular-level model of short segments of amyloid fibrils composed of 6 layers (of ≈ 30 Å length) has recently been described in the literature based on solid state NMR data.^{4,6} However, experimentally imaged and characterized fibrils are typically on the order of several hundred nanometers. This leaves a gap between imaging results and structural models, which prevents us from developing a rigorous understanding of the key physical properties of amyloid fibrils. Specifically, the link between structural features

such as periodic twisting observed at scales of hundreds of nanometers and the underlying atomic structure remains elusive, preventing a direct comparison of structural models with transmission electron microscope (TEM) based imaging of amyloid fibrils.

To resolve this issue, our analysis starts from one layer of the threefolded fibril discussed in Refs. 4 and 6 [structure shown in Fig. 1(b)]. We copy and translate the coordinates of the single layer along the fiber axis N times (where $N = 2, 3 \dots 20, 25, 30, 40$), imposing the typical interstrand distance of the β -sheet configuration $d = 4.8$ Å, where no rotation is imposed between the layer copies ($\theta \approx 0^\circ$). Using the implicit solvent model implemented in the CHARMM force field model (EEF1),⁸ the structures are minimized to relax strain, and then equilibrated at finite temperature. The minimization consists of 10 000 Steepest Descent steps followed by 50 000 Adopted Basis Newton-Raphson method steps. The subsequent equilibration is performed using the Velocity-Verlet algorithm for 1 ns (timestep = 1 fs) at a constant temperature of 300 K. After minimization and relax-

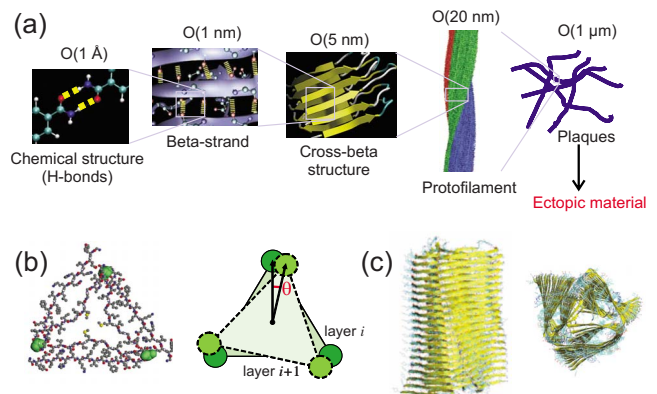


FIG. 1. (Color online) Multiscale representation of the amyloid fibers, from atomistic details to the fiber and plaque scales. (a) Multiscale view of amyloid material (adapted from Ref. 2). (b) Geometry of single layer and twist angle analysis. Left: Atomistic structure of a single layer of the β -amyloid peptide $A\beta(1-40)$. Right: Schematic representation of the structure of two layers, used for the calculation of the twist angle of the fiber. (c) Predicted atomic-level structure of a 20 layer thick amyloid fibril (side view, left; top view, right).

^{a)} Author to whom correspondence should be addressed. Electronic mail: mbuehler@mit.edu. Tel.: +1-617-452-2750. FAX: +1-617-324-4014.

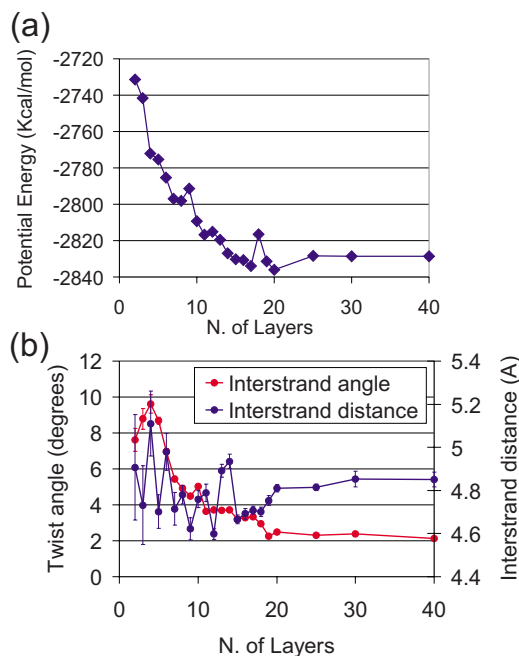


FIG. 2. (Color online) Dependence of energetic and structural (geometric) properties on the number of layers. Panel (a) shows the fiber potential energy as a function of the number of layers. Panel (b) depicts the interstrand twist angle and the distance with the corresponding root mean square deviations computed in the last 200 ps of the relaxation process. The reported values are normalized by the number of layers, N .

ation the geometry of the amyloid fibril converges. Whereas the structure twists slightly during energy minimization, we observe significant twist angle formation during the finite temperature equilibration process. Figure 1(c) displays a sample structure (for $N=20$), clearly showing the twist angle along the fibril axis. The occurrence of the axial twist agrees qualitatively with the published structure of the $A\beta(1-42)$ peptide.⁶

Several explanations for the occurrence of the twist angle have been suggested, including the entropy associated with the backbone degrees of freedom,⁹ the out-of-plane deformation of peptide groups,¹⁰ intrastrand,¹¹ as well as tertiary interactions.¹² Moreover, according to a model published in 2005 by Koh and Tim,¹³ the degree of twist should be determined by the tendency to minimize the surface area of the system. A more recent analysis of the energetic implications of the twist angle in β -sheets structures suggested that the structure is stabilized by entropic contributions associated with an increase in backbone dynamics.¹⁴ Our finding that the twist appears during the finite temperature equilibration phase corroborates this concept¹⁴ and illustrates the importance of entropic contributions.

In order to identify the energetic and structural changes during fiber growth, we systematically calculate the energy associated of amyloid fibrils as a function of the number of layers, where we plot the fibril potential energy normalized by the number of layers [Fig. 2(a)]. We find that short fibrils feature a stronger dependence of the average energy associated with adding a new layer onto an existing nanofibril. However, an energy plateau is reached for fibrils with more than ≈ 20 layers, suggesting that adding new layers to an existing fiber of greater length remains an energetically favorable process that does not depend on the length. The stronger energetic driving force for ultrasmall fibrils may ex-

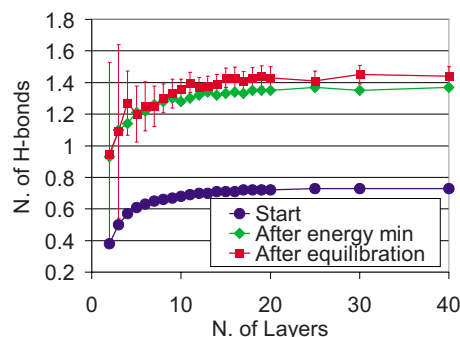


FIG. 3. (Color online) Total number of H-bonds per amino acid (including backbone and side chains), as a function of the number of layers. Results are plotted in the starting, minimized, and relaxed configuration. Error bars correspond to the root mean square deviations in the last 200 ps of the relaxation process. The extrapolated asymptotic value is ≈ 1.42 H-bonds per amino acid. Since the value is >1 , both backbone and side chain mediated H-bonds are formed.

plain the strong propensity toward rapid fibril growth once a basic amyloid nucleus has been formed. We note that the small peaks along the energy profile [e.g., at $N=18$, Fig. 2(a)] are due to the choice of the starting configuration, which can influence the local energy of small structures.

Further analysis of the geometric properties, specifically the twist angle θ and the interlayer distance d , are shown in Fig. 2(b), both as a function of the number of layers N . Both geometric parameters are calculated considering the vector positions of the serine amino acid residues that occupy the corners of the approximated triangles defining the basis of the fiber as shown in Fig. 1(b) (schematic on the right). This choice is motivated by the fact that the positions of the serine residues are least affected by entropic effects that are found on the tails of each chain composing the layers (leading to more fluctuations of the geometry measurements). Similar as in the case of the energy, we find that ≈ 20 layers correspond to a critical fiber length at which the geometric parameters become size independent. The extrapolated values for the interstrand distance and the twist angle are $d \approx 4.85$ Å and $\theta \approx 2.12^\circ$, respectively.

Figure 3 shows the number of H-bonds per amino acid in the fibril (=H-bond density), as a function of the number of layers in the fiber. The analysis shows that the energy minimization step leads to a significant increase in the number of H-bonds. There is also a slight increase in H-bond density during finite temperature equilibration, but it is significantly smaller than during the minimization step. The smaller increase in the twist angle during energy minimization compared with finite temperature equilibration (0.82° versus 1.66° , respectively), and the significant increase in the H-bond density during energy minimization suggests that H-bonds are not critical for twist formation. This observation provides additional support for the hypothesis that twist formation is driven by entropic effects,¹⁴ as discussed above. The extrapolated asymptotic value of the H-bond density is ≈ 1.42 H-bonds per amino acid. This confirms earlier suggestions that amyloid fibrils feature a rather high density of H-bonds, and also reveals that both backbone and side chain H-bonds are formed within the fibril. The existence of a dense array of small clusters of H-bonds [see, e.g., Fig. 1(c)] may be basis of the unusual structural and mechanical properties of this class of macromolecules.¹⁵

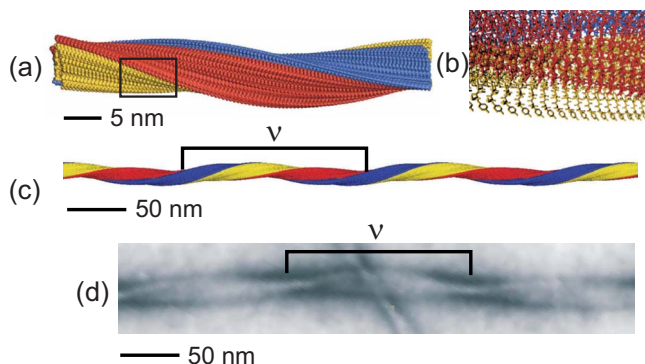


FIG. 4. (Color online) Comparison between the predicted structures [panels (a) and (c); total length=48 and 480 nm, respectively], where panel (b) is a blowup of the region indicated in panel (a) (atoms are colored according to the beta-strand they belong to, where each side of the triangle shown in Fig. 1(b) features a unique color). Panel (d) shows a snapshot of an experimentally studied amyloid fibril. The experimental transmission electron microscope images clearly show the presence of twisted fibers (Ref. 18), in agreement with the simulation predictions. The diameter of the fibrils in experiment and simulation agree well, being around $\approx 7\text{--}8$ nm in both cases. Panel (d) adapted and reproduced from Ref. 19, copyright © 2000 National Academy of Sciences, U.S.A.

The geometrical features extracted from atomistic simulations are now used to build a structural model for larger-scale amyloid fiber structures, by applying simple rotation-translation matrices to reflect the values of d and θ .¹⁶ Two amyloid fiber structures with different lengths (48 and 480 nm) are shown in Figs. 4(a) and 4(c), displaying the formation of a periodically twisted geometry. A visual comparison with an experimental TEM image of the same amyloid fiber type is reported in Fig. 4(d), confirming that the twisted structure is also found *in vitro*. The diameter of the fibrils in experiment and simulation agree well, being around ≈ 8 nm in both cases. To facilitate a quantitative comparison between experiment and simulation, we define the periodicity as the distance between apparent minima in the fibril width (as can be observed in negatively stained transmission electron microscope images). The interstrand twist angle and distance enables us to calculate the periodicity $\nu = 360 \cdot d / \theta \approx 82$ nm, where the corresponding experimental value is $\nu \approx 120 \pm 20$ nm.⁶ This difference between the experimental and predicted values of the fiber periodicity could perhaps be explained by taking into account the fact that the predicted fiber geometry is an extrapolation based on a perfect structure, which does not include any geometric defects in the overall structure. That is, in experimentally measured fibers the presence of local defects may effectively reduce the twist angle, which results in larger periodicity values. Indeed, we have observed that structural (molecular-level) defects in amyloid fibrils can be formed that result in increasing values of ν (this is observed in simulations where the fibril's energy is not completely minimized and the structure is trapped in a local energy minimum).

In summary, our results provide atomistic-level structure predictions for microscale amyloid fiber structures (Fig. 4), and thereby link the atomistic details of small fibrils to the geometric properties of larger ones, through several orders of magnitudes in length scales. The approach used here provides a novel way forward to link the amino acid sequence to structural properties with measurable geometric effects at much larger hierarchical levels in the material. For example, sequence variations could be studied *in vitro* and *in silico* and then their properties could be compared in experiment.¹⁷ Such studies may help to understand fundamental issues related to the geometry of amyloid growth and structure. The properties of predicted amyloid fiber structures could be studied using molecular or coarse-grained simulation approaches, which could result in identifying the stiffness, elasticity and strength properties, for example. Similarly, electronic structure calculations could be utilized to elucidate electronic, magnetic, and optical properties of amyloid fibers.

This research was supported by the Office of Naval Research Grant No. NN-00014-08-01-0844. The authors state that they have no competing financial interests.

- ¹M. Fandrich, M. A. Fletcher, and C. M. Dobson, *Nature (London)* **410**, 165 (2001); C. M. Dobson, *ibid.* **426**, 884 (2003).
- ²M. J. Buehler and Y. C. Yung, *Nature Mater.* **8**, 175 (2009).
- ³R. Nelson, M. R. Sawaya, M. Balbirnie, A. O. Madsen, C. Riekel, R. Grothe, and D. Eisenberg, *Nature (London)* **435**, 773 (2005).
- ⁴A. T. Petkova, Y. Ishii, J. J. Balbach, O. N. Anzutkin, R. D. Leapman, F. Delaglio, and R. Tycko, *Proc. Natl. Acad. Sci. U.S.A.* **99**, 16742 (2002).
- ⁵C. P. Jaronec, C. E. MacPhee, N. S. Astrof, C. M. Dobson, and R. G. Griffin, *Proc. Natl. Acad. Sci. U.S.A.* **99**, 16748 (2002).
- ⁶A. Paravastu, R. D. Leapman, W.-M. Yau, and R. Tycko, *Proc. Natl. Acad. Sci. U.S.A.* **105**, 18349 (2008).
- ⁷D. M. Fowler, A. V. Koulov, W. E. Balch, and J. W. Kelly, *Trends Biochem. Sci.* **32**, 217 (2007); F. Chiti and C. M. Dobson, *Annu. Rev. Biochem.* **75**, 333 (2006).
- ⁸B. R. Brooks, R. E. Bruccoleri, B. D. Olafson, D. J. States, S. Swaminathan, and M. Karplus, *J. Comput. Chem.* **4**, 187 (1983); T. Lazaridis and M. Karplus, *Proteins: Struct., Funct., Genet.* **35**, 133 (1999).
- ⁹C. Chothia, *J. Mol. Biol.* **75**, 295 (1973).
- ¹⁰F. R. Salemme, *Prog. Biophys. Mol. Biol.* **42**, 95 (1983).
- ¹¹P. H. Maccallum, R. Poet, and E. J. Milner-White, *J. Mol. Biol.* **248**, 374 (1995); K. C. Chou, G. Nemethy, and H. A. Scheraga, *ibid.* **168**, 389 (1983).
- ¹²A. S. Yang and B. Honig, *J. Mol. Biol.* **252**, 366 (1995); L. Wang, T. Oconnell, A. Tropsha, and J. Hermans, *ibid.* **262**, 283 (1996).
- ¹³E. Koh and T. Kim, *Proteins* **61**, 559 (2005).
- ¹⁴X. Periolo, A. Rampioni, M. Vendruscolo, and A. E. Mark, *J. Phys. Chem. B* **113**, 1728 (2009).
- ¹⁵S. Keten and M. J. Buehler, *Nano Lett.* **8**, 743 (2008); *Phys. Rev. E* **78**, 061913 (2008); *Phys. Rev. Lett.* **100**, 198301 (2008).
- ¹⁶PDB files of the microscale amyloid fibrils are available from the authors upon request.
- ¹⁷S. Kumar and P. R. LeDuc, *Exp. Mech.* **49**, 11 (2009).
- ¹⁸R. Tycko, *Biochemistry* **42**, 3151 (2003)
- ¹⁹O. N. Anzutkin, J. J. Balbach, R. D. Leapman, N. W. Rizzo, J. Reed, and R. Tycko, *Proc. Natl. Acad. Sci. U.S.A.* **97**, 13045 (2000).